Soft Matter

Rheological dynamics and structural characteristics of supramolecular assemblies of β-cyclodextrin and sulfonic surfactants

Journal:	*Soft Matter*
Manuscript ID	SM-ART-02-2023-000132.R1
Article Type:	Paper
Date Submitted by the Author:	17-Feb-2023
Complete List of Authors:	Bhat, Bhargavi; Texas A&M University, Chemical Engineering Pahari, Silabrata; Texas A&M University System, Chemical Engineering Kwon, Joseph; Texas A&M University System, Akbulut, Mustafa; Texas A&M University, Chemical Engineering;

ARTICLE

Rheological dynamics and structural characteristics of supramolecular assemblies of β-cyclodextrin and sulfonic surfactants

Received 00th January 20xx,
Accepted 00th January 20xx

DOI: 10.1039/x0xx00000x

Bhargavi Bhat[a] , Silabrata Pahari[a], Joseph Sang-Il Kwon[a,c] and Mustafa E. S. Akbulut [a,b,c,*]

Cyclodextrins are highly functional compounds with a hydrophobic cavity capable of forming supramolecular inclusion complexes with various classes of molecules including surfactants. The resultant rich nanostructures and their dynamics are an interesting research problem in the area of soft condensed matter and related applications. Herein, we report novel dynamical supramolecular assemblies based on the complexation of β-cyclodextrin with 3 different sulfonic surfactants, which are sodium hexadecylsulfate, sodium dodecylbenzenesulfonate, and myristyl sulfobetaine. It was observed that a molar ratio of β-cyclodextrin:surfactant / 2:1 was ideal for inducing axial growth and imparting large viscosities in the suspensions. Such complexation processes were accompanied by intriguing nanostructural phase behaviors and rheological properties that were very sensitive to molecular architecture of sulfonic surfactants. The presence of an amino group in the head group of the surfactant allowed for large viscosities that touched 2.4×10^4 Pa.s which exhibited gel-like behavior. In contrast, smaller viscosity values with a lower consistency index were observed when a bulky aromatic ring was present instead. DIC microscopy was used to visually probe the microstructure of the systems with respect to sulfonate molecular architecture. Additionally, surface tension measurements, FTIR and NMR spectroscopy were used to gain insights into the nature of interactions that lead to the complexation and nanostructural characteristics. Finally, mechanics correlating the supramolecular morphologies to the rheological properties were proposed.

Introduction

Supramolecular chemistry entails the study of entities that are held together by weaker non-covalent bonds that are capable of self-assembly and often respond to an external stimulus to form smart materials[1–3]. This field has been inspired heavily by naturally occurring biological materials where this phenomenon is omnipresent[4]. Various noncovalent interactions are involved between the constituents as they rearrange to form energetically favorable configurations such as: π–π stacking, hydrogen bonding, metal-ligand coordination, halogen bonding, hydrophobic interactions, and electrostatic interactions[5,6]. Another key feature to consider is the diversity in the building blocks that can propagate to form a variety of byzantine multidimensional architectures. Some of the materials that have been employed in this domain include: polymers, surfactants, peptides, coordination compounds, nanoparticles, dendrimers[7–10].

Surfactants have often been used in conjunction with a counterion or complexing agent in aqueous suspensions to yield suspensions with interesting rheological behavior, which occurs due to the formation of micellar patterns[11–14]. The primary framework involved in determining the shape that the micelles assemble into is the micellar packing parameter (P), where $P = v_o/al_o$. This quantity can be tuned by varying the length (l_o) and volume (v_o) of the hydrophobic tail or the area (a) of the headgroup[15,16]. When the value of packing parameter lies in between 1/3 and 1/2, axial growth is favored to reduce the end cap energy of the micelle which ultimately yields wormlike micelles that can entangle and yield viscous suspensions[17]. However, in a previous study, we have discussed how non-traditional bilayer-based rods are feasible that can also impart viscoelasticity[18–20]. It is believed that the complexing agent used is capable of tuning the packing parameter of the surfactants via supramolecular assembly to yield interesting nanoarchitectures. So far, several classes of complexing agents have been explored such as salts, carboxylic acids, polyamines, and cyclodextrins[21–23].

Cyclodextrins (CD) refer to a family of cyclic oligosaccharides with fascinating complexation properties that are obtained by enzymatically degrading polysaccharides such as starch. Basic cyclodextrins consist of repeating α-(1,4) linked glucopyranose subunits, where α-CDs, β-CDs and γ-CDs contain 6,7 and 8 units respectively[24,25]. They have increased tremendously in popularity since the 1980s since their application in the food and pharmaceutical industries took off[24]. Their use in drug delivery mitigates several of the key issues associated with solubility of drugs while considering active pharmaceutical

[a] Artie McFerrin Department of Chemical Engineering, Texas A&M University, College Station, TX 77843, USA.
[b] Department of Materials Science and Engineering, Texas A&M University, College Station, TX 77843, USA.
[c] Texas A&M Energy Institute, College Station, TX 77843, USA.
Electronic Supplementary Information (ESI) available: [details of any supplementary information available should be included here]. See DOI: 10.1039/x0xx00000x
* Email: makbulut@tamu.edu

ingredients to increase bioavailability, since the hydrophobic cavity is often large enough to accommodate drugs[26,27]. Furthermore, they tend to pack in cage-type, brick-type or channel-type crystalline lattice assemblies due to their extensive hydrogen bonding network[28–30]. Cyclodextrin-surfactant inclusion complexes and their corresponding packing assemblies have been considered previously[28,31,32]. In particular, work by Jiang *et al*.[33,34] has given interesting reports regarding vesicle and microtube formations of β-CD with sodium dodecyl sulfate. However, little is known about the rheological dynamics of these systems. Furthermore, there is limited literature on how the molecular details of long-chain sulfonic surfactants can alter the supramolecular characteristics of their complexes with cyclodextrins.

In this work, we study the rheological behavior of the supramolecular combination of β-CD with three different sulfonic surfactants: Sodium hexadecylsulfate, sodium dodecylbenzenesulfonate, and myristyl sulfobetaine. A detailed analysis of the viscosity and viscoelastic properties for this system was conducted. DIC microscopy was used to gauge the microstructure of the system which is what ultimately gives rise to those rheological properties. The complexation was explained using NMR and FTIR spectroscopy and a mechanism for the suspension structure was proposed. Cyclodextrins and surfactants are often used in the biomedical space and in cosmetic formulations and hence, it is useful to gain fresh perspectives on the colloidal and rheological behavior of such systems aside from general scientific advancement towards obtaining a better understanding of structure-property relationships of binary supramolecular complexes involving cyclodextrins.

Materials and Methods

Materials and assembly of supramolecular mixtures

The chemical structures of the sulfonic surfactants used in the study as well as β-cyclodextrin (β -CD) are presented in Fig. 1. Sodium hexadecylsulfate and sodium dodecylbenzenesulfonate were procured from TCI Chemicals (Tokyo, Japan). β-CD was obtained from Alfa Aesar (Haverhill, MA, USA) and 3-(N,N-Dimethylmyristylammonio)propane sulfonate, also known as myristyl sulfobetaine, was purchased from Sigma Aldrich (St. Louis, MO, USA). The suspensions were prepared by mixing the constituents in ultrapure water obtained from a Barnstead water purification system (Thermo Fisher Scientific, Waltham, MA) using magnetic stirring to ensure even dispersion. In each of the prepared suspensions, the concentration of surfactant was kept constant at 50 mM and the concentration of β-CD was varied from 50 mM-100 mM depending on the molar ratio selected. The primary focus of the paper has been on the case where the β-CD concentration was 100 mM.

Fig. 1: The chemical structures of the constituents used in the supramolecular assemblies.

Rheological Measurements

The overall procedure in place for the rheological studies is comparable to that of previous studies[18,35,36]. Viscosity *versus* shear rate was measured in each case using a rheometer (Haake RS 1, Thermo Fisher Scientific, Waltham, MA, USA) equipped with a 60 mm diameter parallel plate (PP60 Ti). The shear rate was increased logarithmically and stepwise (15 steps) from 0.003 s^{-1} to 100 s^{-1}, while setting the gap between the plates constant at 1 mm. Measurements were recorded by keeping the shear rate steady at each step for 10 seconds and subsequently averaging the viscosity across that time interval. The measurements were repeated thrice for each sample to ensure statistical reliability.

For viscoelasticity measurements, another rotational rheometer (DHR-2, TA Instruments, New Castle, DE, USA) possessing a steel parallel plate geometry of 40 mm diameter was used. In this case, 1 mm gap setting between the plates was employed as well. Storage and loss modulus measurements for all samples were conducted at a strain amplitude of 0.4% by logarithmically sweeping the frequency from 0.001 Hz to 20 Hz at room temperature. This specific value of strain was selected by conducting amplitude sweep measurements and deciding the limit of linear viscoelasticity for the samples. The samples were made to endure strain ranging from 0.01-100% while recording the moduli. The strain value at which the storage modulus begins to change drastically is the selected limit.

Structural Analysis using DIC microscopy, AFM, and Small-Angle X-ray Scattering

Differential Interference Contrast (DIC) microscopy is a technique that uses linearly polarized light to introduce sufficient contrast and effectively image samples in cases where the samples do not have much inherent contrast[33]. In this work, an Axio Imager M2 optical microscope with DIC imaging (Zeiss, Oberkochen, Germany) was employed to characterize the microstructural entanglements of the studied suspensions. Drops of unstained samples were dropped on to glass slides and placed under the objective for imaging.

Additionally, AFM (Dimension Icon, Bruker) was used to record a magnified perspective of the microtubes. The setting used was tapping mode with 2 nm diameter silicon nitride probes attached to the cantilever. 2μm×2μm images were captured at a scan rate of 0.5 Hz and analyzed thereafter.

As an additional characterization method to comprehend the nanoscale structures, Small Angle X-ray scattering of the suspensions was undertaken using the instrument Rigaku S-MAX3000 (Rigaku Corporation, Tokyo, Japan) at the Soft Matter Facility, Texas A&M University. The suspensions with a concentration of 50 mM surfactant and 100 mM β-CD were loaded into 3 mm capillary tubes using a syringe and then sealed with wax. The measurements were taken for 15-30 minutes in vacuum after which the data was analyzed.

Spectroscopic analysis of supramolecular assemblies by FTIR and NMR

Attenuated total reflectance-Fourier transform infrared (FT-IR) spectroscopy (Nicolet iS5, Thermo Fisher Scientific, Waltham, MA) was used as a method to investigate the interactions that

lead to formation of supramolecular inclusion complexes. The spectra were obtained by sweeping the wavenumber from 1000 cm^{-1} to 4000 cm^{-1} with triplicate repeats, with focus remaining on the region from 3200 cm^{-1} to 3700 cm^{-1}. Baseline correction was incorporated for the suspension samples to take into account the dominance of water in the spectra. Additionally, proton nuclear magnetic resonance (^{1}H-NMR) spectroscopy was used to determine the hydrogen bonding interactions in the suspensions using an Avance Neo 400 Mhz instrument (Bruker, Billerica, MA). For this experiment, diluted versions of all the suspensions were prepared in deuterium oxide (TCI Chemicals, Tokyo, Japan) to reduce the water peak in the spectra.

Surface Tension Measurements

Pendant drop tensiometry was utilized to obtain the surface tension values for pure surfactant solutions as well as the β-CD/surfactant suspensions. The surface tension curves for the surfactants are presented in Fig. S1. While studying the complexed systems, the concentration of surfactants was kept at 2 mM and that of β-CD was 4 mM. The low concentration was chosen to ensure that gel formation does not occur, while maintaining the ratio between the constituents as β-CD:surfactant / 2:1. Axisymmetric drop images were obtained with a house-made goniometer and subsequently analyzed by using ImageJ software (National Institutes of Health [NIH], Bethesda, MD, USA). In particular, the pendant drop plugin was used to fit the droplet shape to a gouette pendant and obtain the surface tension value. Each measurement was repeated thrice and averaged for statistical reliability.

Results and Discussion

In order to determine the optimum molar ratio that enhances the rheological properties the most, β-CD/surfactant were combined at various molar ratios as shown in Fig. 2. It is quite evident that the molar ratio of β-CD:surfactant / 2:1 is most effective for all the three surfactants. In the case of Fig. 2(a) and Fig. 2(c), we can see that opaque gels are obtained at this particular molar ratio that do not succumb to gravity upon vial inversion, which has often been used as a measure of determining viscoelasticity of a substance[37]. Even in the case of Fig. 2(b), we can see that this particular ratio has more viscoelastic behavior compared to the others since the viscoelastic liquid sticks to the walls of the vial while sliding down. The difference in macroscopic behavior between different molar ratios is most apparent in the case of Fig. 2(c), wherein the suspensions at other molar ratios depict water-like behavior, and fall immediately upon vial inversion.

Fig. 2: Photos depicting macroscopic phase behavior of (a) β-CD/SHS (b) β-CD/SDBS (c) β-CD/MSB suspensions. In each instance, the molar ratio of β-CD:surfactant varies as 1:1, 2:1, 2:3 from left to right. The photos were taken immediately after vial inversion.

Steady shear viscosity behavior of the β-CD and surfactant suspensions

The steady shear rheological response for the three β-CD/surfactant systems of interest at the different molar ratios that were considered are displayed in Fig. 3. The β-CD/MSB system had the most impressive viscosity behavior at neutral pH for a molar ratio of 2:1, with the value reaching 2.4×10^4 Pa.s at a shear rate of 0.003 s^{-1} followed by the β-CD/SHS system which also displayed a relatively high viscosity of 2428 Pa.s at the same shear rate and molar ratio. This supports the observation that stiff gels were observed for these compositions. In contrast, the β-CD/SDBS suspension which displayed viscoelastic flow rather than gel-like behavior has a viscosity which is orders of magnitude lower than the others. Furthermore, there is a good correlation between what was visually observed in the macroscopic phase images and the viscosity versus shear-rate analysis. The starkest change upon differing the molar ratio was exhibited by the β-CD/MSB suspension, wherein the viscosity differed by a 5-order magnitude. The sensitivity of the rheological properties to the internal composition is quite apparent which is why the molar ratio of β-CD:surfactant / 2:1 was used for all further tests since it displayed the most impressive rheological properties.

Fig. 3: Viscosity versus shear rate curves at different molar ratios for (a) β-CD/SHS (b) β-CD/SDBS (c) β-CD/MSB suspensions. The concentration of surfactant is 50 mM in each case and the concentration of cyclodextrin is varied. The error bars represent standard error from mean.

Generally, in surfactant systems that have been predominantly discussed in literature so far, the viscosity versus shear rate curves exhibits a Newtonian plateau at very low shear rates. This information can then be used to determine the zero-shear viscosity for that particular system. However, in the case of the β-CD/surfactant complexes studied in this work, the fluid appears to be completely shear thinning in the range of measurement. Hence, it becomes more appropriate to consider the use of the Ostwald de Waele equation which is used for the shear thinning regime of non-Newtonian fluids[38]. The aforementioned equation is as follows:

$$\eta = K(\dot{\gamma})^{n-1}$$

where η and $\dot{\gamma}$ are the viscosity and shear rate respectively, K is the consistency index and n is the power law index. Table 1 represents the parameters obtained by fitting the viscosity versus shear rate curves at the molar ratio of 2:1 (β-CD:surfactant) to the above equation. The corresponding fitted curves are shown in the supplementary information (Fig. S2).
The value of n is a measure of the structural properties of the system as a whole[39]. A given system is considered to be shear thinning when the value of n is less than unity, with a smaller value indicating stronger shear thinning behavior. Based on this fact, we observe that the β-CD/MSB suspension has the most shear thinning tendency of the three studied suspensions. The consistency index has been linked to the characteristics of the individual fibers that make up the suspension, with a larger K-value being indicative of a larger axial ratio of the nanorod[39,40].

The β-CD/MSB suspension has the highest K-value followed closely by β-CD/SHS which also corresponds to generally higher values of viscosity as is observed above. Having high values of consistency is considered useful while preparing cosmetic formulations as it can help mitigate undesirable flocculation and sedimentation[41].

Table 1: The values obtained for consistency index (K) and power law index (n) by fitting the steady-shear viscosity curves to power law model for the β-CD/surfactant systems.

Suspension Formula	Consistency Index (K)	Power Law Index (n)
β-CD/SHS	14.88±0.05	0.19±0.02
β-CD/SDBS	2.09±0.01	0.26±0.01
β-CD/MSB	15.81±0.16	-0.04±0.04

Dynamic viscoelastic properties of the β-CD/surfactant suspension systems

The viscoelastic behavior of the suspensions at room temperature are quantified by measurement of the storage and loss modulus as can be seen in Fig. 4. Additional viscoelastic measurements are presented in the supplementary information (Fig. S3). The β-CD/SDBS and β-CD/SHS suspensions display characteristics of a typical Maxwellian fluid, which is usually characterized by a terminal region and an elastic region[42]. The value of the storage modulus changes ever so slightly on the log-log scale in the elastic region, which can be seen for these two systems. The low-frequency dependence of the elastic modulus alludes towards a relatively strong nanostructural network and gel-like characteristics[43]. Another interesting parallel with Maxwellian behavior lies in the fact that both the loss moduli reach a minimum value. But, the loss modulus does not diminish as swiftly as is expected for pure Maxwellian fluids. This is probably because there may be multiple relaxation times in the system rather than one and thus, it may be more appropriate to describe this behavior by the Maxwell-Weichert model which is a generalized version of the Maxwell model[44].

In the terminal region, the angular frequency is very low and hence, the time scales are long enough for strained entanglements to be resolved by reptative motion of the constituent chains along their contour. The end of this region is marked by the relaxation time, which quantifies the structural integrity of the nanoarchitecture of the viscosifying network[42]. However, it is likely that this region is reached at very large time scales for both the β-CD/SDBS and β-CD/SHS suspensions and is hence not accessible in the range of measurement. Another region that is seldom mentioned in literature is the "breathing regime", which occurs at very small timescales and reflects individual segment dynamics in a network[45,46]. Herein, the loss modulus crosses over the relaxation modulus for a second time, which is when the breathing regime is said to occur. This phenomenon is observed for the β-CD/SDBS and β-CD/MSB systems after a relatively low angular frequency of 10 rad/s. An interesting contrast when compared to typical aqueous wormlike micelles lies in the fact that the breathing regime is usually only observed after 10^5 rad/s [45].

Fig. 4: Storage(G') and Loss Modulus(G'') curves for β-CD/surfactant systems measured from 0.001-20 Hz (0.0063-125.6 rad/s). The concentration of surfactant is 50 mM and β-CD is 100 mM.

The case of β-CD/MSB poses an unconventional yet intriguing rheological behavior. The values of G' are highest, indicating strongest elastic networks despite having almost equal viscous behavior as presented by the G" values. The frequency dependence of these parameters for this system is low, since both curves possess a very small slope, which is a key characteristic of "true" gels[47,48]. Another peculiar observation is the fact that both the terminal regime and breathing regime are accessible in the range of measurement for this sample. A possible explanation is that the higher elasticity of the sample allows for stress to be relaxed more conveniently thus leading to a lower relaxation time[49].

Structural Characteristics of the β-CD/surfactant suspension systems

DIC microscopic images are presented in Fig. 5 in order to visually probe the architecture that ultimately imparts rheological properties to the suspensions. The presence of long rod-like structures with length scales touching several microns can be identified for all the samples. It is these rods that form an entangled mesh which is capable of trapping solvent molecules and enhancing the viscosity and viscoelasticity of the mixture, in a manner similar to that of typical wormlike micelles that have frequently been discussed in literature as a viscosifying agent[17,50,51]. It is important to note the variations in packing amongst the 3 samples which yield different bulk rheological properties.

Interestingly, the rods in the case of β-CD/MSB and β-CD/SHS suspensions are longer and more tightly packed than in the case of β-CD/SDBS. It is possible that the zwitterionic nature of MSB surfactant allows for closer packing of the headgroups and reduces the end cap energies sufficiently to facilitate long-range axial growth, due to fewer repulsions between the headgroups. In the case of SHS surfactant, a long carbon tail and small head group is likely the reason for ordered growth of long rods. However, the SDBS surfactant has a bulky benzyl headgroup and relatively shorter tail, which probably does not allow for analogous ordered growth to occur. An additional micrograph at more magnification further iterates the observation of shorter rods (Fig. S4). It can also be observed that the packing of these rods is less ordered in this case, probably due to the relatively fluid-like nature of this combination as compared to the other two.

Fig. 5: DIC optical micrographs at 40x of (a)β-CD/SHS, (b)β-CD/SDBS, and (c)β-CD/MSB suspensions. The scale bars are 20 μm for all micrographs.

The nature and morphology of the micellar growth can clearly be correlated with the strength of the rheological properties discussed in the previous section. The mesh formed by longer rods with more order in their network lead to enhanced viscosities and gel-like behavior in aqueous assemblies with cyclodextrin, as observed for β-CD/MSB and β-CD/SHS systems. However, the fact that the rods can be clearly perceived under

an optical microscope indicates that the rods have a diameter larger than 10 nm, which is usually the thermodynamically feasible upper diameter limit of wormlike micelles[52,53]. AFM microscopy for the case of β-CD/MSB also shows rod-like morphology with diameters touching 130 nm (Fig. 6). Hence, it is apparent that the morphology needs to be considered in a manner different from traditional surfactant-based worms, which are monolayered cylinders. This will be discussed further in a later section.

Fig. 6: AFM micrograph of β-CD/MSB.

Complexation mechanism of the β-CD/surfactant suspension systems

To better understand the driving forces that contribute to the self-assembly of the β-CD/surfactant complexes, various concepts were considered. The lack of any charged headgroups at neutral pH and the presence of extensive hydroxyl groups in the molecular structure of cyclodextrin make hydrogen bonding a likely candidate for driving complexation and nanotubule formation. As a means to detect these bonds, the IR spectra region that covers the O-H stretching region is presented in Fig. 7, since involvement of hydroxyl groups in hydrogen bonding would cause peak shifts in this very region[54]. The prominent hydroxyl peak in the case of β-CD is visible at 3295 cm^{-1}, which shifts to approximately 3394 cm^{-1} in the case of β-CD/surfactant suspensions. The shift to higher wavenumber is most likely due to the insertion of the surfactant tail in the cyclodextrin ring, which disrupts the native hydrogen bonding network of pure β-CD. Furthermore, the repulsions due to charges on the headgroups of the surfactant molecules are most likely contributing to weakening of the hydroxyl bond structure in native β-CD[55].

^{1}H-NMR has frequently been cited as another effective technique for detecting dynamic hydrogen bonding interactions in cyclodextrin complexes[56,57]. The approximate positions of the hydrogen groups in the conical structure being studied are shown in Fig. 8. In the case of β-CD, the H-3 and H-5 bonds are considered to be in the interior of the cyclodextrin ring[58]. Therefore, the introduction of a hydrophobic moiety inside the ring or any other changes to these bonds should result in a significant chemical shift in the NMR spectra of the β-CD/surfactant suspensions (in the region corresponding to β-CD) as compared to pure cyclodextrin[59,60]. Indeed, this is what is observed for all the three complexed systems as shown in Fig. 8. The signals for both the H-3 and H-5 bonds shifted upfield due to increased electron shielding, with a numerical shift value (δ) of -0.0551 ppm to -0.2484 ppm. The complete chemical shift data table is presented in the supplementary information (Table S1). Similar shifts in this range have been used previously as a means to confirm hydrogen bonding[56,58,61]. In all the cases, $|\delta_{H\text{-}5}| > |\delta_{H\text{-}3}|$ which lets us know that complete inclusion of the surfactant is taking place rather than partial inclusion[56].

Fig. 7: ATR-FTIR spectra of (a) β-CD/surfactant suspensions (b) Plain β-CD

The surface tension values of plain as well as complexed surfactant solutions were determined at room temperature as another means to confirm the interaction between the constituents and are tabulated in Table 2. The surface tension of plain water is expected to be around 72 mN/m at 25°C[62]. One of the key properties of a good surfactant is its ability to decrease the surface tension of water due to relatively lower intermolecular forces between surfactant and water molecule, which is what is observed numerically. However, in all three cases, the addition of β-CD causes the surface tension to rise once again. This difference is most apparent in the case of β-CD+MSB since zwitterionic surfactants have the primary advantage of larger surface activity as compared to anionic surfactants[63]. It is likely that the hydrophobic tail which was initially able to participate at the air-water interface has now been attracted to the hydrophobic cavity of the cyclodextrin molecule, resulting in reduced surface activity of the surfactant.

Fig. 8: ^{1}H-NMR spectra of β-CD, β-CD/SHS, β-CD/SDBS, β-CD/MSB

Work done by Angelova et. al[64] has previously discussed this phenomenon, in which a surface-active drug polymyxin B (PMB) lost its surface activity upon the addition of β-CD in the system due to complexation.

Table 2: Surface tension values of surfactant solutions and β-CD(4 mM)/surfactant(2 mM) complexes

Surface Tension (mN/m)	SHS	SDBS	MSB
Surfactant Only	46.05±2.96	46.83±3.11	34.32±1.67
Surfactant + β-CD	52.77±2.03	56.88±2.73	52.66±2.11

Discussion

It is essential to comprehend how the β-CD/surfactant inclusion complexes end up forming multimolecular structures that lead to enhanced rheological properties. In order to assess the nanoscale structure, SAXS analysis was performed for the samples. Herein, multilayered nanotubules with diameters reaching 250 nm were identified for all of the samples. The detailed analysis is provided in the supplementary information (Fig. S5, Fig. S6). Fig. 9 is a visual representation of what is likely occurring in these systems, leading to the tubular geometry. The internal cavity of the cyclodextrin molecule is hydrophobic, due to the C-H bonds which are directed inwards. The release of highly energetic water present inside the cyclodextrin cavity is what entropically and energetically favors the aqueous self-assembly of the system[28]. This cavity attracts the hydrophobic surfactant tail to form an inclusion complex which is stabilized by many Van der Waals interactions. It is well established that 2 cyclodextrin molecules usually encapsulate the surfactant tail when the chain length is greater than 12 carbon atoms, as shown in the schematic[28]. This reinforces the fact that starkly

enhanced properties were observed at this particular molar ratio in our analysis so far.

Jiang et. al[33,34] have discussed how similar complexes of sodium dodecyl sulfate (SDS) and β-CD are able to form lamellar bilayer structures that then self-assemble into other shapes such as vesicles and microtubes. Interestingly, this phenomenon has been exploited to design protein-mimetic giant capsids and ordered membranes[65,66]. Microtubular assemblies for complexes consisting of β-CD and myristyl sulfobetaine (MSB) have also been considered[67]. Based on the experimental data, we are able to conclude that in this case, the building blocks consists of inclusion complexes that form crystalline bilayer membranes as shown in the schematic. In terms of the micellar packing parameter (P), the value seems to be increasing because of cyclodextrin to allow for axial growth. The growth is being propelled by the external hydroxyl groups on the cyclodextrin molecules which are trying to maximize the hydrogen bonding network. The charge on the surfactant molecule helps prevent precipitation in such a scenario[68]. Subsequently, the β-CD/surfactant sheets may be folding up to minimize contact between hydrophobic tails at the edge of a bilayer sheet to water in a manner similar to lipid bilayers in aqueous conditions[34]. The "annular ring" tubes thus formed can potentially have much larger diameters than traditional wormlike micelles.

Fig. 9: Schematic illustration showing complexation and nanoarchitecture in β-CD/surfactant suspensions (Molar ratio β-CD:surfactant / 2:1)

Sufficient concentrations of the aforementioned tubes would allow for mesh formation in aqueous suspensions due to overlaps and entanglements. It has frequently been discussed in literature how such meshes can effectively trap and immobilize liquid molecules, thus leading to larger values of viscosity and moduli[69]. The variations in rheological properties observed while different surfactants are being considered may be due to the differences in the hydrophilic head group. Sodium dodecylbenzenesulfonate has a smaller chain length and a bulky head group which may lead to more steric repulsions and hence less favorable conditions for packing and axial growth. On the other hand, myristyl sulfobetaine is zwitterionic, with a net-neutral headgroup which tends to have fewer electrostatic repulsions hence promoting close packing and large viscosities.

Conclusions

In this work, supramolecular combinations of a cyclic oligosaccharide, β-cyclodextrin with 3 distinct sulfonic surfactants (Sodium hexadecylsulfate, sodium dodecylbenzenesulfonate and myristyl sulfobetaine) are considered. One of the novel aspects of the study is the fact that rheology of long-chained surfactants using β-CD as a complexing agent rather than the typically used cosurfactants/salts that promote axial growth is examined. All the surfactants considered have variations in their head and tail groups which propagate on to the rheological properties in an interesting manner. The ideal molar ratio between the constituents was identified to be β-CD:surfactant / 2:1 since the enhancement of aqueous rheology was the most stark at this ratio. It was concluded that the interactions holding the constituents in place is likely hydrogen bonding. Using DIC microscopy and AFM as visual tools, extremely long rods with relatively large diameters were spotted. Upon utilizing SAXS as additional tool, it could be determined that the morphology may be different from wormlike micelles that are commonly reported for surfactant systems with high viscosity values and rather, multi-layered nanotubules are actually omnipresent in the suspension.

Nanotubular architecture for the purpose of rheological modification is not a commonly discussed phenomenon and has only been mentioned in a few select works[18,70,71]. Hence, more in-depth insights are necessary into the entropic conditions that make these configurations stable. Also, it is likely that the same concepts of scission and reptation that are used to explain stress relaxation in wormlike micelles cannot be applied here. Therefore, alternative theories need to be considered for these cases. Cyclodextrins are biologically viable compounds which is why they are often used in the food, pharmaceutical and cosmetic industries. On the other hand, surfactants are also ubiquitous in biomedical products and in the consumer goods space. It is thus an essential research problem to comprehend the colloidal and rheological behavior of such supramolecular dynamic binary complexes.

Author Contributions

Bhargavi Bhat: Investigation, Writing- Original draft preparation, Conceptualization; Silabrata Pahari: Formal analysis; Joseph Sang-Il Kwon: Writing – review & editing; Mustafa Akbulut: Writing- Reviewing and Editing, Supervision, Conceptualization

Conflicts of interest

There are no conflicts to declare.

Acknowledgements

This material is based upon work supported by the U.S. Department of Energy, Office of Fossil Energy under Award Number DE-FE0031778. The authors acknowledge the assistance of the Image Analysis Laboratory, Texas A&M Veterinary Medicine & Biomedical Sciences, RRID: SCR_022479.

References

1 F. Huang and O. A. Scherman, *Chem. Soc. Rev.*, 2012, **41**, 5879–5880.

2 X. Yan, F. Wang, B. Zheng and F. Huang, *Chem. Soc. Rev.*, 2012, **41**, 6042–6065.

3 K. Liu, Y. Yao, Y. Kang, Y. Liu, Y. Han, Y. Wang, Z. Li and X. Zhang, *Sci. Rep.*, 2013, **3**, 1–7.

4 D. A. Uhlenheuer, K. Petkau and L. Brunsveld, *Chem. Soc. Rev.*, 2010, **39**, 2817–2826.
5 L. Barrientos, S. Miranda-Rojas and F. Mendizabal, *Int. J. Quantum Chem.*, 2019, **119**, 1–16.
6 B. Roy, P. Bairi and A. K. Nandi, *RSC Adv.*, 2014, **4**, 1708–1734.
7 H. J. Sun, S. Zhang and V. Percec, *Chem. Soc. Rev.*, 2015, **44**, 3900–3923.
8 S. Datta, M. L. Saha and P. J. Stang, *Acc. Chem. Res.*, 2018, **51**, 2047–2063.
9 A. Noro, M. Hayashi and Y. Matsushita, *Soft Matter*, 2012, 8, 6416–6429.
10 J. Meid, F. Dierkes, J. Cui, R. Messing, A. J. Crosby, A. Schmidt and W. Richtering, *Soft Matter*, 2012, **8**, 4254–4263.
11 M. S. Bakshi and K. Singh, *J. Colloid Interface Sci.*, 2005, **287**, 288–297.
12 M. E. Cates and S. J. Candau, *Journal of Physics: Condensed Matter*, 1990, **2**, 6869–6892.
13 Z. Chu, Y. Feng, X. Su and Y. Han, *Langmuir*, 2010, **26**, 7783–7791.
14 S. Pahari, B. Bhadriraju, M. Akbulut and J. S. il Kwon, *J. Colloid Interface Sci.*, 2021, **600**, 550–560.
15 I. S. Oliveira, M. Lo, M. J. Araújo and E. F. Marques, *Soft Matter*, 2019, **15**, 3700–3711.
16 P. Sun, F. Lu, A. Wu, L. Shi and L. Zheng, *Soft Matter*, 2017, **13**, 2543.
17 C. A. Dreiss, in *Wormlike Micelles: Advances in Systems, Characterisation and Applications*, 2017, pp. 1–8.
18 B. Bhat, S. Pahari, S. Liu, Y.-T. Lin, J. Kwon and M. Akbulut, *Colloids Surf. A Physicochem. Eng. Asp.*, 2022, **654**, 130067.
19 J. Yang, *Curr. Opin. Colloid Interface Sci.*, 2002, **7**, 276–281.
20 S. Pahari, S. Liu, C. H. Lee, M. Akbulut and J. S. il Kwon, *Soft Matter*, 2022, **18**, 5282–5292.
21 M. A. da Silva, V. Calabrese, J. Schmitt, K. M. Z. Hossain, S. J. Bryant, N. Mahmoudi, J. L. Scott and K. J. Edler, *Soft Matter*, 2020, **16**, 4887–4896.
22 T. Tixier, H. Tabuteau, A. Carrière, L. Ramos and C. Ligoure, *Soft Matter*, 2010, **6**, 2699–2707.
23 J. Penfold, R. K. Thomas and P. X. Li, *J. Colloid Interface Sci.*, 2015, **449**, 167–174.
24 G. Crini, *Chem. Rev.*, 2014, **114**, 10940–10975.
25 E. M. M. del Valle, *Process Biochemistry*, 2004, **39**, 1033–1046.
26 M. E. Davis and M. E. Brewster, *Nat. Rev. Drug Discov.*, 2004, **3**, 1023–1035.
27 J. Zhang and P. X. Ma, *Adv. Drug Deliv. Rev.*, 2013, **65**, 1215–1233.
28 L. dos Santos Silva Araújo, G. Lazzara and L. Chiappisi, *Adv. Colloid Interface Sci.*, 2021, **289**, 102375.
29 H. Wang, J. C. Wagner, W. Chen, C. Wang and W. Xiong, *Proceedings of the National Academy of Sciences*, 2020, **117**, 23385–23392.
30 R. Puliti, C. A. Mattia and L. Paduano, *Carbohydr. Res.*, 1998, **310**, 1–8.
31 H. Mwakibete, R. Cristantino, + D M Bloor, E. Wyn-Jones and J. F. Holzwarth, *Langmuir*, 1995, **11**, 57–60.
32 A. González-Pérez, R. S. Dias, T. Nylander and B. Lindman, *Biomacromolecules*, 2008, **9**, 772–775.
33 L. Jiang, Y. Peng, Y. Yan, M. Deng, Y. Wang and J. Huang, *Soft Matter*, 2010, **6**, 1731–1736.
34 L. Jiang, Y. Peng, Y. Yan and J. Huang, *Soft Matter*, 2011, **7**, 1726–1731.
35 S. Liu, Y. T. Lin, B. Bhat, K. Y. Kuan, J. S. I. Kwon and M. Akbulut, *RSC Adv.*, 2021, **11**, 22517–22529.
36 B. Bhat, S. Liu, Y. Lin, M. L. Sentmanat, J. S.-I. Kwon and M. Akbulut, *PLoS One*, 2021, **16**, e0260786.
37 S. C. Karunakaran, B. J. Cafferty, K. S. Jain, G. B. Schuster and N. v. Hud, *ACS Omega*, 2020, **5**, 344–349.
38 R. P. Chhabra, *Non-Newtonian Fluids: An Introduction*, 2008.
39 A. I. Koponen, *Cellulose*, 2020, **27**, 1879–1897.
40 D. Tatsumi, S. Ishioka and T. Matsumoto, *Journal of Society of Rheology, Japan*, 2002, **30**, 27–32.
41 C. A. P. Moraes, E. P. G. Arêas and M. V. R. Velasco, *Cosmetics*, 2017, **4**, 27.
42 M. In, in *Giant Micelles*, eds. R. Zana and E. W. Kaler, CRC Press, 2007.
43 M. M. Alam, Y. Sugiyama, K. Watanabe and K. Aramaki, *J. Colloid Interface Sci.*, 2010, **341**, 267–272.
44 B. Babaei, A. Davarian, K. M. Pryse, E. L. Elson and G. M. Genin, *J. Mech. Behav. Biomed. Mater.*, 2016, **55**, 32–41.
45 N. R. Agrawal, X. Yue and S. R. Raghavan, *Langmuir*, 2020, **36**, 6370–6377.
46 M. S. Turner and E. Cates, *Linear Viscoelasticity of Living Polymers: A Quantitative Probe of Chemical Relaxation Times*, 1991, vol. 7.
47 G. Lorenzo, N. Zaritzky and A. Califano, in *Polymers for Food Applications*, Springer International Publishing, 2018, pp. 481–507.
48 M. Alloncle and J. L. Doublier, *Top Catal.*, 1991, **5**, 455–467.
49 D. Long and P. Sotta, *Rheol. Acta*, 2007, **46**, 1029–1044.
50 Y. Lin, X. Han, J. Huang, H. Fu and C. Yu, *J. Colloid Interface Sci.*, 2009, **330**, 449–455.
51 S. A. Rogers, M. A. Calabrese and N. J. Wagner, *Curr. Opin. Colloid Interface Sci.*, 2014, **19**, 530–535.
52 S. R. Raghavan and E. W. Kaler, *Langmuir*, 2001, **17**, 300–306.
53 Y. Feng, Z. Chu and C. A. Dreiss, in *Smart Wormlike Micelles*, 2015, pp. 1–6.
54 S. Kubo and J. F. Kadla, *Biomacromolecules*, 2005, **6**, 2815–2821.
55 C. Zhou, X. Cheng, Q. Zhao, Y. Yan, J. Wang and J. Huang, *Langmuir*, 2013, **29**, 13175–13182.
56 F. B. T. Pessine, A. Calderini and G. L. Alexandrino, in *Magnetic Resonance Spectroscopy*, 2012, pp. 1–30.
57 S. K. Upadhyay and G. Kumar, *Chem. Cent. J.*, 2009, **3**, 9.

58 X. Zhong, C. Hu, X. Yan, X. Liu and D. Zhu, *J. Mol. Liq.*, 2018, **272**, 209–217.

59 H.-J. Schneider, F. Hacket, V. Rüdiger and H. Ikeda, *Chem. Rev.*, 1998, **98**, 1755–1786.

60 J. Wang, Q. Li, S. Yi and X. Chen, *Soft Matter*, 2017, **13**, 6490–6498.

61 R. Zhao, C. Sandström, H. Zhang and T. Tan, *Molecules*, 2016, **21**, 372.

62 N. B. Vargaftik, B. N. Volkov and L. D. Voljak, *Surface Tension of Seawater Journal of Physical and Chemical Reference Data*, 1983, **12**, 20007.

63 R. Sarkar, A. Pal, A. Rakshit and B. Saha, *J. Surfactants Deterg.*, 2021, **24**, 709–730.

64 A. Angelova, C. Ringard-Lefebvre and A. Baszkin, *Journal of Colloid and Interface Science*, 1999, **212**, 275–279.

65 S. Yang, Y. Yan, J. Huang, A. v. Petukhov, L. M. J. Kroon-Batenburg, M. Drechsler, C. Zhou, M. Tu, S. Granick and L. Jiang, *Nat. Commun.*, 2017, **8**, 15856.

66 J. Landman, S. Ouhajji, S. Prévost, T. Narayanan, J. Groenewold, A. P. Philipse, W. K. Kegel and A. v Petukhov, *Sci. Adv.*, 2018, **4**, 2375–2548.

67 L. Jiang, Y. Yan and J. Huang, *Soft Matter*, 2011, **7**, 10417–10423.

68 H. Dodziuk, *Cyclodextrins and Their Complexes: Chemistry, Analytical Methods, Applications*, John Wiley and Sons, 2006.

69 J. Hua Shi, X. Yang Liu, J. Liang Li, C. S. Strom and H. Yao Xu, *J. Phys. Chem. B*, 2009, **113**, 4549–4544.

70 L. Jia, D. Lévy, D. Durand, M. Impéror-Clerc, A. Cao and M. H. Li, *Soft Matter*, 2011, **7**, 7395–7403.

71 S. H. Kim, F. Nederberg, R. Jakobs, J. P. K. Tan, K. Fukushima, A. Nelson, E. W. Meijer, Y. Y. Yang and J. L. Hedrick, *Angewandte Chemie - International Edition*, 2009, 48, 4508–4512.

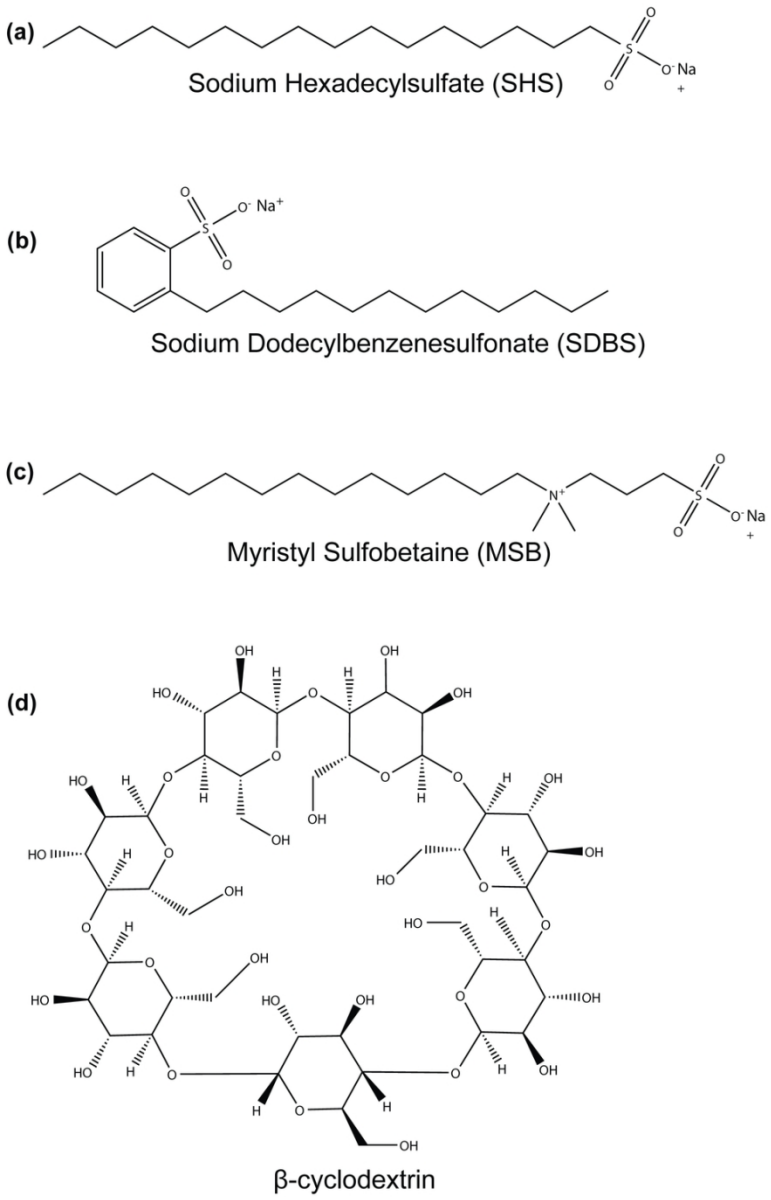

Fig. 1: The chemical structures of the constituents used in the supramolecular assemblies.

82x128mm (300 x 300 DPI)

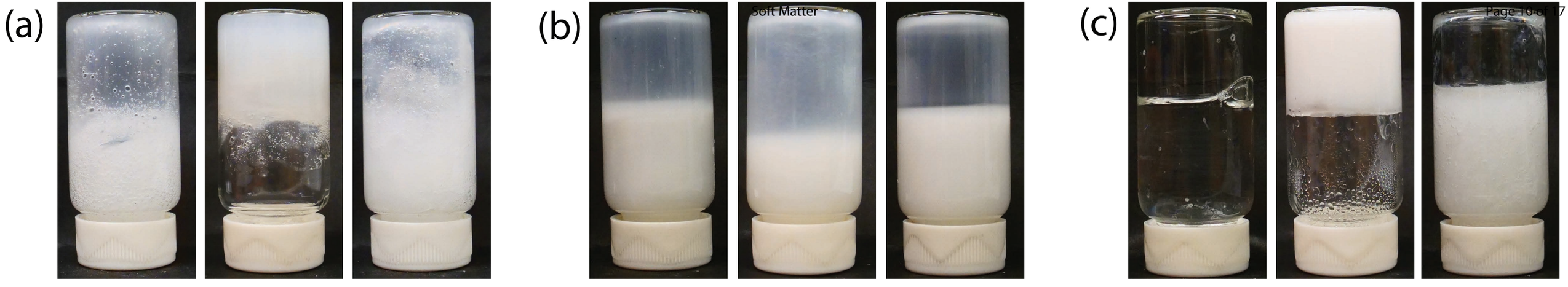
(a)
(b)
(c)

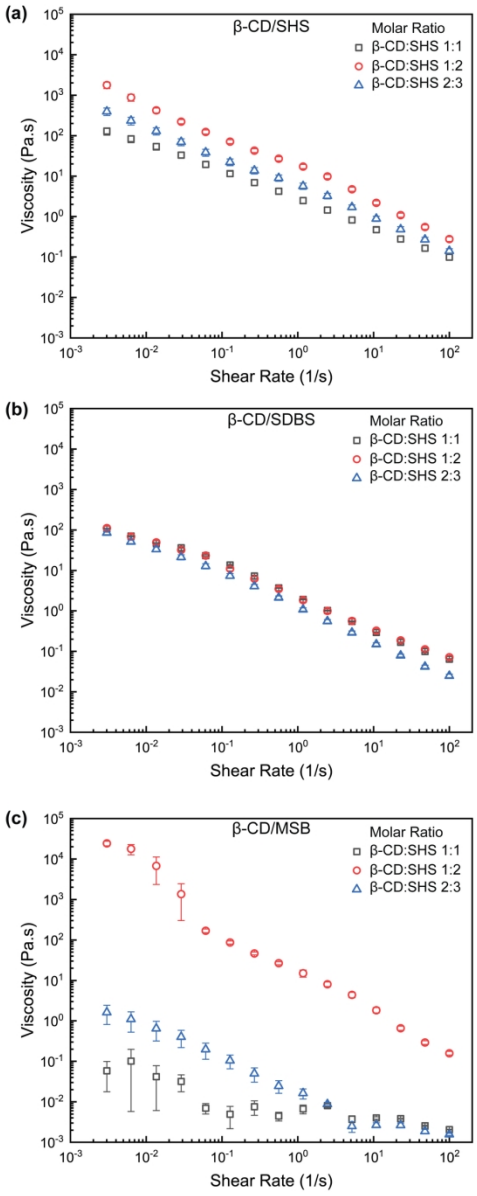

Fig. 3: Viscosity versus shear rate curves at different molar ratios for (a) β-CD/SHS (b) β-CD/SDBS (c) β-CD/MSB suspensions. The concentration of surfactant is 50 mM in each case and the concentration of cyclodextrin is varied. The error bars represent standard error from mean.

82x206mm (300 x 300 DPI)

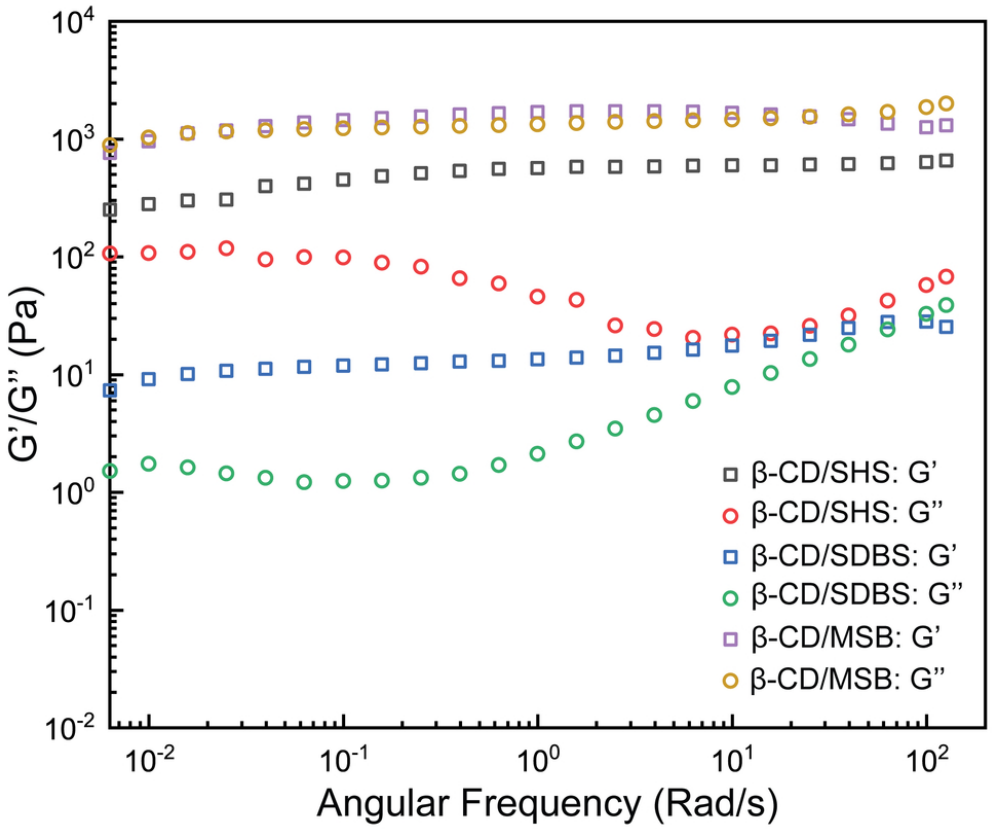

Fig. 4: Storage(G') and Loss Modulus(G'') curves for β-CD/surfactant systems measured from 0.001-20 Hz (0.0063-125.6 rad/s). The concentration of surfactant is 50 mM and β-CD is 100 mM.

82x70mm (300 x 300 DPI)

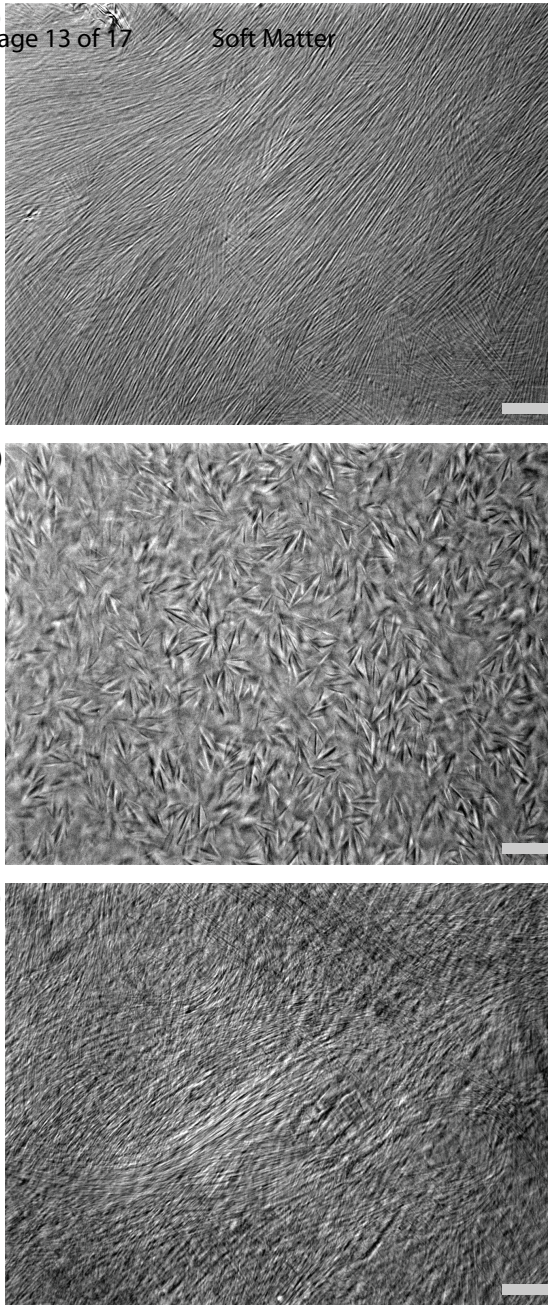
(a)
(b)
(c)

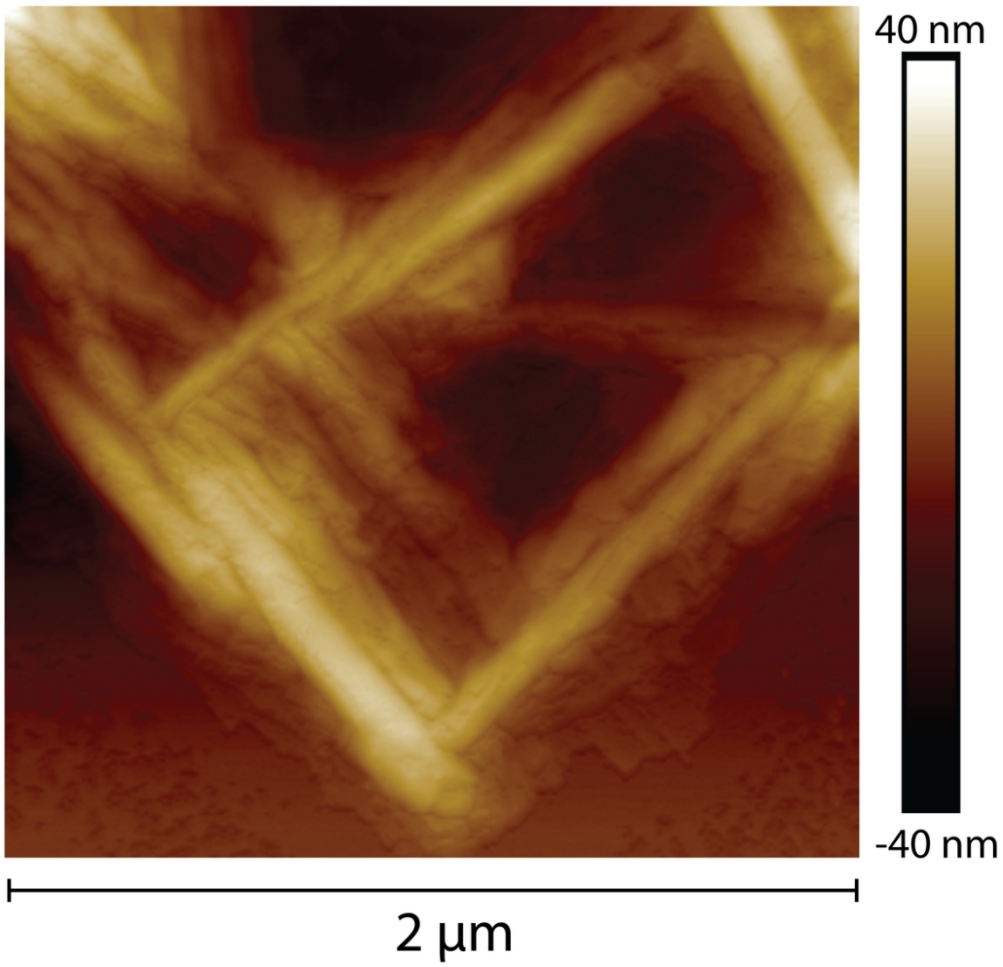

Fig. 6: AFM micrograph of β-CD/MSB.

99x95mm (300 x 300 DPI)

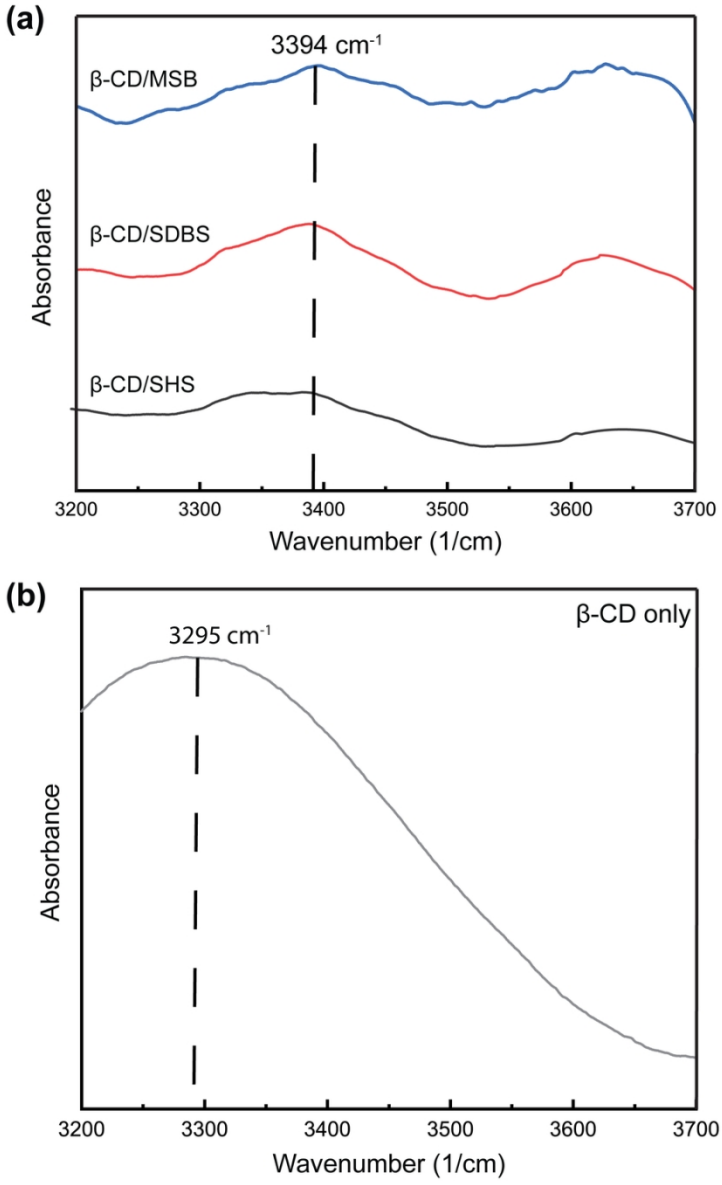

Fig. 7: ATR-FTIR spectra of (a) β-CD/surfactant suspensions (b) Plain β-CD

80x130mm (300 x 300 DPI)

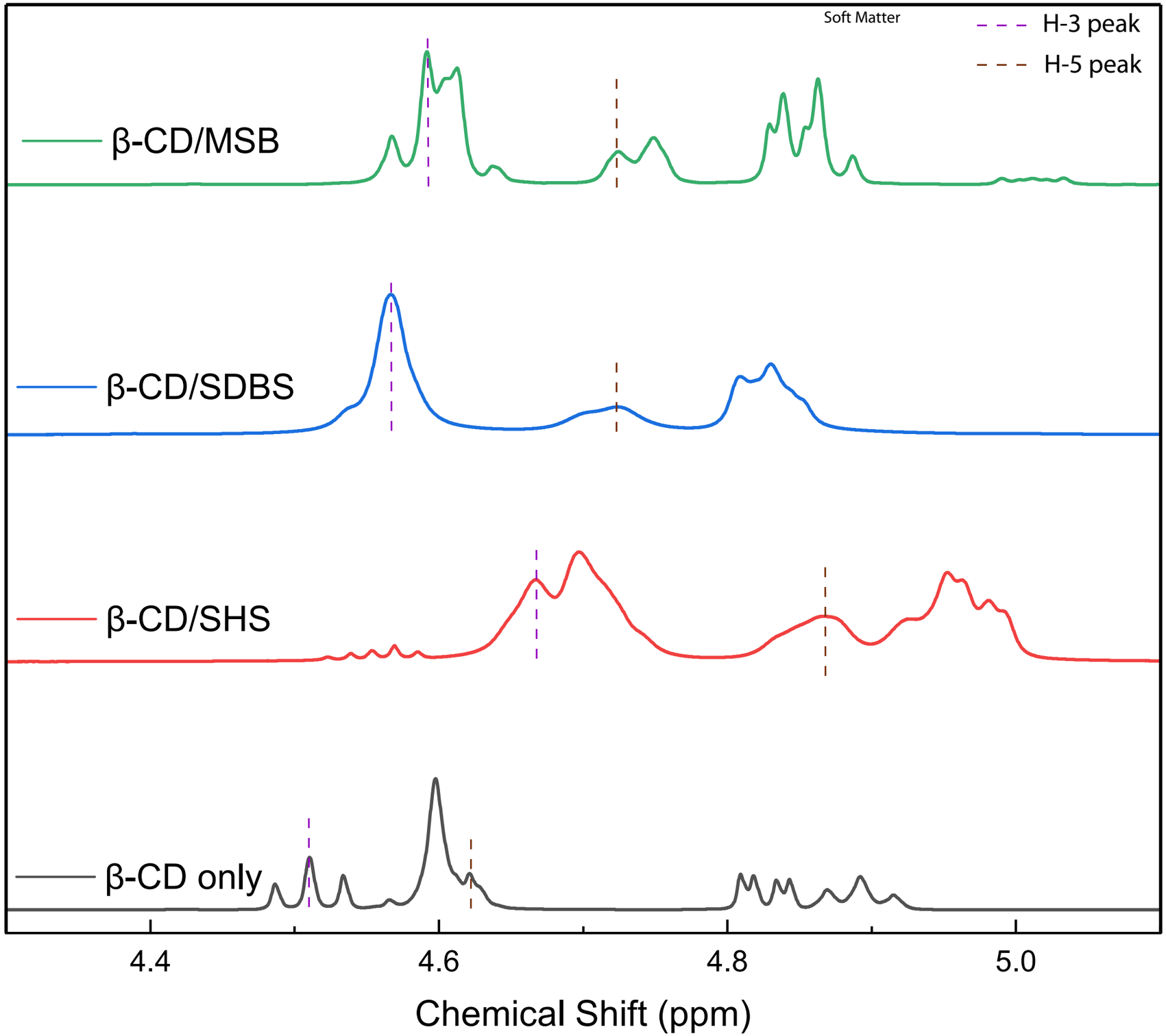
H-3 peak
H-5 peak
β-CD/MSB
β-CD/SDBS
β-CD/SHS
β-CD only
4.4
4.6
4.8
5.0
Chemical Shift (ppm)

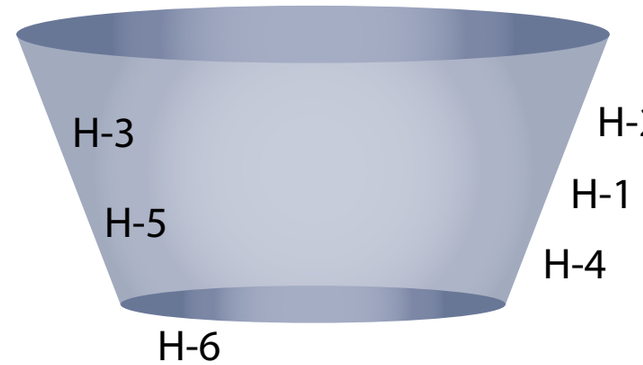
H-3
H-2
H-1
H-5
H-4
H-6

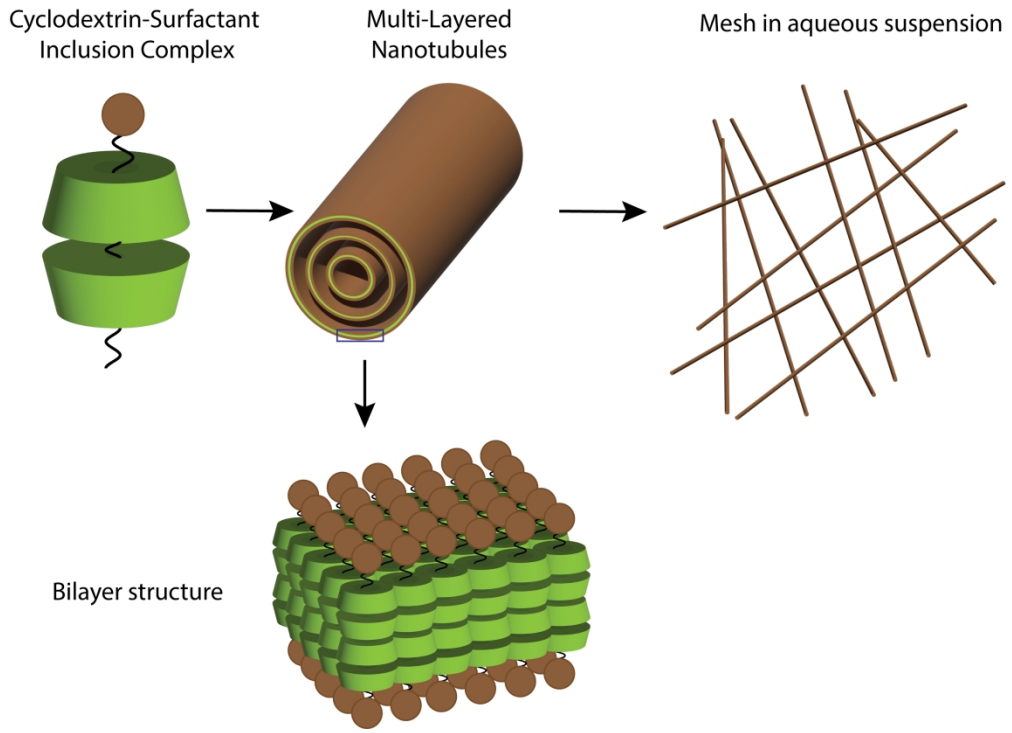

Fig. 9: Schematic illustration showing complexation and nanoarchitecture in β-CD/surfactant suspensions (Molar ratio β-CD:surfactant / 2:1)

247x178mm (300 x 300 DPI)